JOURNAL OF GEOPHYSICAL RESEARCH, VOL. 91, NO. D6, PAGES 6671–6681, MAY 20, 1986

Numerical Advection by Conservation of Second-Order Moments

MICHAEL J. PRATHER[1]

Center for Earth and Planetary Physics, Harvard University, Cambridge, Massachusetts

A new, accurate, and nondiffusive method for three-dimensional advection of trace species is presented. The method preserves tracer structures by conserving the second-order moments of the spatial distribution of tracer during advection. Tracer concentrations are represented by separate, second-order polynomials within each grid box. This second-order moments method has been shown, in typical tests for advective schemes, to be equal or superior to presently available methods in terms of absolute accuracy, numerical diffusion, and computational cost.

1. INTRODUCTION

Simulation of the spatial distribution and chemical interaction of trace elements throughout the atmosphere and ocean often requires accurate numerical advection of trace species. In many such "tracer-transport" problems it is assumed that the global velocity field is given and that the "tracer" is transported passively along with the mean flow. Furthermore, the abundance of these tracers is regarded to be sufficiently small so that physical and chemical transformations which produce or destroy tracers do not change the general mass field. This paper presents a new, stable and nondispersive method for numerical advection of tracers in three dimensions. The focus is on atmospheric applications and on a class of scientific problems ranging from regional studies of air pollution [e.g., *Seinfeld*, 1975; *Mahlman and Sinclair*, 1977; *Eliassen*, 1980; *Graedel and Schiavone*, 1981; *McRae et al.*, 1982; *McRae and Seinfeld*, 1983] to global simulations of natural and anthropogenic trace gases [e.g., *Mahlman and Moxim*, 1978; *Holton*, 1981; *Levy et al.*, 1982; *Steed et al.*, 1982; *Tung*, 1982; *Fung et al.*, 1983; *Ko et al.*, 1984].

The continuity equation for a fluid with a three-dimensional velocity field (u, v, w) may be written as

$$\frac{\partial \rho}{\partial t} = -\frac{\partial \rho u}{\partial x} - \frac{\partial \rho v}{\partial y} - \frac{\partial \rho w}{\partial z} \tag{1}$$

where $\rho(x, y, z)$ is the fluid density in grams per cubic centimeter. The continuity equation at a fixed point in space for a trace constituent of the fluid is then

$$\frac{\partial f}{\partial t} = -u\frac{\partial f}{\partial x} - v\frac{\partial f}{\partial y} - w\frac{\partial f}{\partial z} + p \tag{2}$$

where $f(x, y, z)$ describes the mixing ratio of tracer by mass (gram of tracer per gram of fluid). The term p (gram of tracer per gram of fluid per second) represents local sources, photochemical production and loss, or other mechanisms capable of removing the tracer from the mean flow (for example, precipitation). The following discussion focuses on inert tracers ($p = 0$). An important consequence of defining f in terms of mass mixing ratio is that convergence or divergence of the background fluid ($\partial\rho/\partial t \neq 0$) does not directly lead to changes in f.

A clear requirement of an acceptable numerical advection scheme is that the total amount of tracer should be conserved with high accuracy. Further, the scheme should provide a straightforward method for calculating and averaging chemical transformations involving several trace species over specified volumes. This approach leads naturally to a grid of boxes which fills the entire space. The continuity equations are then replaced with ones relating $\bar{\rho}$ (mean density) and $\bar{f}$ (mean tracer mixing ratio) for each grid box to the flux across the sides of the box. For the one-dimensional grid of length X, (1) and (2) become

$$\frac{\partial \bar{\rho}}{\partial t} = (u^-\rho^- - u^+\rho^+)/X \tag{3}$$

$$\frac{\partial \bar{\rho}\bar{f}}{\partial t} = (u^-\rho^- f^- - u^+\rho^+ f^+)/X \tag{4}$$

where the superscript plus and minus refer to the leading and trailing edges of the grid box. A major difficulty with (4) is the determination of f at the boundaries (f^+, f^-) in terms of the mean values ($\bar{f}$).

Coupling of adjacent grid boxes should generally occur only through explicit advection or diffusion. Chemical processes within one box may be calculated independently of those occurring in neighboring boxes. Methods which integrate chemical budgets by implicitly assuming continuity of chemical processes (that is, p in equation (21)) across the grid are undesirable and often dangerous. The local photochemical environment may change discontinuously by orders of magnitude: for example, clear skies versus clouds and rain, or moist polluted boundary layers versus clean dry air above.

The paper by *Russell and Lerner* [1981] provides a major advance in advection schemes suitable to chemical tracer models. They coupled a basic upstream algorithm with a least squares procedure determining the slope of the tracer distribution within each grid box. This "slopes" scheme has all of the desired properties for use in chemical tracer models, but it is more diffusive than some of the numerical schemes reviewed in recent studies [*Chock and Dunker*, 1983; *Smolarkiewicz*, 1983, 1984; *Schere*, 1983; *Schneider*, 1984]. A comparison of the capabilities of different algorithms shows that each scheme has its advantages and that no one method is most advantageous under all conditions. For example, high-order polynomial schemes or pseudospectral methods are nondiffusive but often produce negative fluctuations in the tracer concentration, which must be filled in after the advective step. Flux-corrected methods and the slopes scheme can maintain

[1]Now at NASA Goddard Institute for Space Studies, New York, New York.

Paper number 6D0087.
0148-0227/86/006D-0087$05.00

positive tracer concentrations during advection, but they tend to numerically disperse steep gradients in the tracer distribution. Furthermore, high-order schemes which are less diffusive often require small time steps for stability and accuracy.

The method proposed here, conservation of second-order moments, appears to include the best qualities of most other methods: (1) conservation of tracer; (2) positive tracer concentration can be maintained during advection; (3) stable for large time steps up to the Courant limit (that is, the entire box is moved in one time step); (4) accurate when compared with analytic solutions for a nondivergent flow; and (5) high effective grid resolution (that is, resolves and advects structures on the order of the grid size).

The method used in this paper is not related to the second-moments technique proposed by *Egan and Mahoney* [1972]. Their procedure describes the tracer distribution as a number of small, discrete rectilinear clumps of tracer, at most one per box, which move as rigid objects both within and between boxes. It does not allow for continuous distribution of tracer within each box and does not include the necessary cross terms. The new second-order moments method is not a classical "second-order" polynomial advection scheme; its accuracy compares favorably with fourth-order differencing schemes. (See *Russell and Lerner* [1981] for comparison of first-order moments with fourth-order polynomial schemes). The new approach to advection of tracers is straightforward and does not involve free parameters, unphysical velocity fields [e.g., *Smolarkiewicz*, 1983], or iterative steps. It is based on *Russell and Lerner*'s [1981] idea of upstream advection with slopes.

In section 2, upstream transport and second-order tracer distributions are described. The moments of the tracer distribution about the center of a grid box are formally defined and are related to the polynomial distribution $f(x, y, z)$ in section 3. Section 3 presents the formulae which describe how the moments of a grid box are decomposed into a unique set of moments centered about each subbox and how they are reassembled into new grid boxes. Section 4 gives a one-dimensional example of tracer transport and derives limits necessary to maintain positive tracer concentrations. Section 5 examines analytically the accuracy and stability of this method and presents numerical experiments testing the effective resolution. The second-order moments method is compared with other methods for numerical advection of tracers in section 6.

2. Upstream Advective Transport

Upstream methods traditionally employ a staggered grid with f evaluated at the center of each grid box and (u, v, w) defined at the boundaries, as in (3) and (4) [e.g., *Haltiner and Williams*, 1980, p. 130]. This technique is mathematically equivalent to treating the grid boxes as volumes of uniform concentration, integrating the appropriate volume from the upwind box (that is, $u\,\Delta t$), adding it to the primary box (which has had a corresponding fraction of its volume sent downwind), and then thoroughly mixing within the box. *Russell and Lerner* [1981] noted that within each grid box the tracer concentrations need not be uniform but could include gradients of tracer concentration. They formulated the advection step therefore as an integral in which the flux of material entering a box in a given time step is calculated by integrating over the tracer distribution in the upstream box. After each advective step the slope of the tracer distribution is reevaluated from the different subvolumes which comprise the new grid box. This technique is employed here. Consider the case in which the tracer mixing ratio is represented globally by a continuous second-order polynomial, as in (5). Upstream advection, which is equivalent to a translation or rotation of coordinates, would preserve this tracer distribution if second-order moments were conserved.

Each grid box is treated as a separate entity with a continuous internal distribution of tracer and with an inevitable discontinuity across the boundaries between boxes. The tracer mixing ratio is expressed as a second-order polynomial in three dimensions,

$$f(x, y, z) = a_0 + a_x x + a_{xx}x^2 + a_y y + a_{yy}y^2 + a_z z + a_{zz}z^2 + a_{xy}xy + a_{yz}yz + a_{xz}xz \qquad (5)$$
$$0 \le x \le X \qquad 0 \le y \le Y \qquad 0 \le z \le Z$$

within a rectilinear grid box of volume $V = XYZ$. The inclusion of cross terms is essential and makes the formulation independent of coordinate rotation. The total amount of fluid R and of tracer M_0 are given by

$$R = \int_0^X \int_0^Y \int_0^Z \rho(x, y, z)\, dx\, dy\, dz$$
$$M_0 = \int_0^X \int_0^Y \int_0^Z f(x, y, z)\rho(x, y, z)\, dx\, dy\, dz \qquad (6)$$

The fluid density is assumed to be uniform within the volume V so that $R = \rho V$. Furthermore, in the following derivations I shall adopt the convenience of setting ρ equal to unity everywhere. The reader is advised to remember that volume integrals are actually density integrals over the fluid mass contained in the grid box and that the tracer distribution $f(x, y, z)$ is tied to the background fluid. This difference will become important, as noted earlier, only if there is a change in the mass of a grid box during the advection scheme. I will then consider the effective volume to have changed along with the mass and will adjust the length of the box in the appropriate dimension.

The calculated advection of a tracer for one time step with the upstream algorithm involves, first, the decomposition of a grid box into two or more rectilinear subboxes. The volume (mass) of each subbox corresponds to the fraction of the original box which would either be advected to an adjacent grid box or would remain in the original grid box. Each subunit retains the original, second-order polynomial distribution of tracer $f(x, y, z)$ but will have new, local moments with respect to its center of mass. Then the advected subunits are gathered within their destination grid box and a new tracer distribution of the same form $f(x, y, z)$ is derived from the moments of the subunits.

The numerical scheme conserves the total tracer abundance (zeroth-order moment), the mean slope of tracer distribution in the three dimensions (three first-order moments), and the curvature in the tracer distribution, including cross terms (six second-order moments). With storage and transport of only zeroth-order moments this method is equivalent to a regular upstream algorithm. With zeroth- and first-order moments it can be shown to be equivalent to *Russell and Lerner*'s [1981] least squares slopes scheme.

The conservation of second-order moments has all of the advantages of the basic upstream method: it is stable in general for large time steps; if necessary, mean tracer values may be kept positive by eliminating transport of subunits with negative tracer; grid box volumes may fluctuate; and the local chemical transformation of tracers is readily integrated over individual grid boxes.

3. Derivation of Second-Order Moments

The moments of the distribution $f(x, y, z)$, as defined in (5), are given by the decomposition of f into orthogonal polynomials over the volume $V = XYZ$:

$$f(x, y, z) = m_0K_0 + m_xK_x + m_{xx}K_{xx} + m_yK_y + m_{yy}K_{yy} + m_zK_z + m_{zz}K_{zz} + m_{xy}K_{xy} + m_{yz}K_{yz} + m_{xz}K_{xz} \quad (7)$$

In this notation the constants m_i are the moment coefficients, and the functions $K_i(x, y, z)$ are orthogonal functions such that

$$\int K_iK_j\, dV = 0 \qquad (i \neq j) \quad (8)$$

for all combinations of i and j equal to 0, x, xx, y, yy, z, zz, xy, xz, and yz. We selected the following set of orthogonal polynomials with rational coefficients,

$$\begin{aligned} K_0 &= 1 \\ K_x(x) &= x - X/2 \\ K_{xx}(x) &= x^2 - Xx + X^2/6 \\ K_y(y) &= y - Y/2 \\ K_{yy}(y) &= y^2 - Yy + Y^2/6 \\ K_z(z) &= z - Z/2 \\ K_{zz}(z) &= z^2 - Zz + Z^2/6 \\ K_{xy}(x, y) &= (x - X/2)(y - Y/2) \\ K_{yz}(y, z) &= (y - Y/2)(z - Z/2) \\ K_{xz}(x, z) &= (x - X/2)(z - Z/2) \end{aligned} \quad (9)$$

with normalizing factors,

$$\begin{aligned} \int {K_x}^2\, dV &= VX^2/12 \\ \int {K_{xx}}^2\, dV &= VX^4/180 \\ \int {K_y}^2\, dV &= VY^2/12 \\ \int {K_{yy}}^2\, dV &= VY^4/180 \\ \int {K_{xy}}^2\, dV &= VX^2Y^2/144 \end{aligned} \quad (10)$$

and with parallel results for K_z, K_{zz}, K_{xz}, and K_{yz}. Moments S_i may be defined therefore from $f(x, y, z)$ by

$$\begin{aligned} S_0 &= \int dV\ f(x, y, z)K_0 = m_0V \\ S_x &= (6/X) \int dV\ f(x, y, z)K_x(x) = m_xVX/2 \\ S_{xx} &= (30/X^2) \int dV\ f(x, y, z)K_{xx}(x) = m_{xx}VX^2/6 \\ S_y &= (6/Y) \int dV\ f(x, y, z)K_y(y) = m_yVY/2 \\ S_{yy} &= (30/Y^2) \int dV\ f(x, y, z)K_{yy}(y) = m_{yy}VY^2/6 \\ S_{xy} &= (36/XY) \int dV\ f(x, y, z)K_{xy}(x, y) = m_{xy}VXY/4 \end{aligned} \quad (11)$$

again, with parallel results for S_z, S_{zz}, S_{xz}, and S_{yz}. The normalization above has been chosen for computational convenience and results in all moments having the same units: mass of tracer. The coefficients of the polynomial expansion in (5) are a linear combination of the moment coefficients,

$$\begin{aligned} a_{xx} &= m_{xx} \qquad a_{yy} = m_{yy} \qquad a_{zz} = m_{zz} \\ a_{xy} &= m_{xy} \qquad a_{yz} = m_{yz} \qquad a_{xz} = m_{xz} \\ a_x &= m_x - m_{xx}X - m_{xy}Y/2 - m_{xz}Z/2 \\ a_y &= m_y - m_{yy}Y - m_{xy}X/2 - m_{yz}Z/2 \\ a_z &= m_z - m_{zz}Z - m_{xz}X/2 - m_{yz}Y/2 \\ a_0 &= m_0 - m_xX/2 - m_yY/2 - m_zZ/2 + m_{xx}X^2/6 + m_{yy}Y^2/6 \\ &\quad + m_{zz}Z^2/6 + m_{xy}XY/4 + m_{yz}YZ/4 + m_{xz}XZ/4 \end{aligned} \quad (12)$$

In the derivations which follow, advection will be restricted to the two-dimensional problem involving only x and y coordinates. I shall focus on the problem of transport, and thus decomposition of moments, for one dimension at a time, assuming that multidimensional advection may be treated in separate steps (see discussion following this derivation). Given a velocity in the x direction of c and a time step of t, I require that the right-hand section of the box, defined by

$$X - ct \leq x \leq X \qquad 0 \leq y \leq Y \qquad 0 \leq z \leq Z \quad (13)$$

be removed from its present grid box and added to the adjacent one on its right. Remember that z may be substituted for y (and similarly, Z for Y) to include the moments in three dimensions.

The first step in upstream transport of second-order moments occurs when the moments of the primary grid box S_i are decomposed into the moments of the fraction of the box to be transported, as defined in (13) above ($S_i{}^R$ for the case $c > 0$), and those which remain ($S_i{}^L$) in the volume

$$0 \leq x \leq X - ct \qquad 0 \leq y \leq Y \qquad 0 \leq z \leq Z \quad (14)$$

(Note here that superscripts L and R refer to the left and right sides of the original grid box.) The new moments and their coefficients, $m_i{}^R$ and $m_i{}^L$, are defined in terms of totally new orthogonal functions, $K_i{}^R$ and $K_i{}^L$, which are defined over the new local volumes $V^R = ctYZ$ and $V^L = (X - ct)YZ$.

$$\begin{aligned} {K_0}^L &= {K_0}^R = 1 \\ {K_x}^L &= x - (X - ct)/2 \qquad {K_x}^R = x - (2X - ct)/2 \\ {K_{xx}}^L &= x^2 - (X - ct)x + (X - ct)^2/6 \\ {K_{xx}}^R &= x^2 - (2X - ct)x + (X - ct)X + (ct)^2/6 \\ {K_y}^L &= {K_y}^R = y - Y/2 \\ {K_{yy}}^L &= {K_{yy}}^R = y^2 - Yy + Y^2/6 \\ {K_{xy}}^L &= [x - (X - ct)/2](y - Y/2) \\ {K_{xy}}^R &= [x - (2X - ct)/2](y - Y/2) \end{aligned} \quad (15)$$

New local moment coefficients may be derived, following some tedious algebra:

$$\begin{aligned} {m_0}^R &= m_0 + \bar{K}_x{}^R m_x + \bar{K}_{xx}{}^R m_{xx} \\ {m_x}^R &= m_x + 2\bar{K}_x{}^R m_{xx} \\ {m_{xx}}^R &= m_{xx} \\ {m_y}^R &= m_y + \bar{K}_x{}^R m_{xy} \\ {m_{yy}}^R &= m_{yy} \\ {m_{xy}}^R &= m_{xy} \end{aligned} \quad (16)$$

where $\bar{K}$ is the average value of the original orthogonal polynomial over the new subinterval.

$$\begin{aligned} \bar{K}_x{}^L &= -ct/2 & \bar{K}_x{}^R &= (X - ct)/2 \\ \bar{K}_{xx}{}^L &= ct(2ct - X)/6 & \bar{K}_{xx}{}^R &= (X - ct)(X - 2ct)/6 \end{aligned} \tag{17}$$

The moments S_i in the transported subinterval

$$\alpha = \alpha^R = ct/X = V^R/V \tag{18}$$

are given then by

$$\begin{aligned} S_0{}^R &= \alpha[S_0 + (1 - \alpha)S_x + (1 - \alpha)(1 - 2\alpha)S_{xx}] \\ S_x{}^R &= \alpha^2[S_x + 3(1 - \alpha)S_{xx}] \\ S_{xx}{}^R &= \alpha^3 S_{xx} \\ S_y{}^R &= \alpha[S_y + (1 - \alpha)S_{xy}] \\ S_{yy}{}^R &= \alpha S_{yy} \\ S_{xy}{}^R &= \alpha^2 S_{xy} \end{aligned} \tag{19}$$

The moments corresponding to (19) for the remaining, left-hand portion of the grid box are calculated with the appropriate $\bar{K}^L$ from (17).

$$\begin{aligned} S_0{}^L &= (1 - \alpha)[S_0 - \alpha S_x - \alpha(1 - 2\alpha)S_{xx}] \\ S_x{}^L &= (1 - \alpha)^2(S_x - 3\alpha S_{xx}) \\ S_{xx}{}^L &= (1 - \alpha)^3 S_{xx} \\ S_y{}^L &= (1 - \alpha)(S_y - \alpha S_{xy}) \\ S_{yy}{}^L &= (1 - \alpha)S_{yy} \\ S_{xy}{}^L &= (1 - \alpha)^2 S_{xy} \end{aligned} \tag{20}$$

Grid boxes are divided into rectilinear subintervals which have local moments defined with respect to each subinterval, not with respect to the original box.

The final step in advection involves the addition of moments from two adjacent boxes into a new grid box. Transformation between the local orthogonal functions ($K_i{}^L$ and $K_i{}^R$) and the new orthogonal basis set for the combined box is tedious but straightforward. The resulting moments may be expressed as

$$\begin{aligned} S_0 &= S_0{}^R + S_0{}^L \\ S_x &= \alpha S_x{}^R + (1 - \alpha)S_x{}^L + 3[(1 - \alpha)S_0{}^R - \alpha S_0{}^L] \\ S_{xx} &= \alpha^2 S_{xx}{}^R + (1 - \alpha)^2 S_{xx}{}^L \\ &\quad + 5\{\alpha(1 - \alpha)(S_x{}^R - S_x{}^L) + (1 - 2\alpha)[(1 - \alpha)S_0{}^R - \alpha S_0{}^L]\} \\ S_y &= S_y{}^R + S_y{}^L \\ S_{yy} &= S_{yy}{}^R + S_{yy}{}^L \\ S_{xy} &= \alpha S_{xy}{}^R + (1 - \alpha)S_{xy}{}^L + 3[(1 - \alpha)S_y{}^R - \alpha S_y{}^L] \end{aligned} \tag{21}$$

where

$$\alpha = \alpha^R = V^R/(V^R + V^L) \tag{22}$$

Dividing a volume into submoments by (19) and (20) followed by the reconstitution of the original volume by (21) results in conservation of the original moments. These formulae apply universally to all velocity fields, remembering that α in (21) refers to the fraction of total fluid mass which is contributed by the right-hand (that is, positive direction) subinterval.

I have shown thus how to partition the grid boxes and their moments, to transport them downstream, and to recombine the pieces into a new grid box with new moments. The necessary boundary conditions must specify the tracer mixing ratio along all upwind boundaries. The total number of moments per grid interval is three for a one-dimensional model, six for a two-dimensional model, and 10 in three dimensions. (Remember to substitute z for y in order to derive all the moments.) No previous history of the tracer distribution is required; advection calculations may begin instantly from any initial spatial distribution of tracer. However, all moments must be initialized or stored to start a calculation. It should be emphasized that the time integration for upstream moments methods is always explicit, forward marching. An encoding of this algorithm into FORTRAN is given in the Figure 1.

The method described here applies directly to one-dimensional transport in a three-dimensional grid. For a three-dimensional wind field the explicit approach would be to divide the grid box by successive partitioning into 2^3 subboxes and then simultaneously to transport seven of these subboxes into neighboring boxes. This method appears to be analytically tedious and computationally expensive for both storage and time requirements, but it might have advantages for vectorized computers with I/O (input/output) limitations.

The approach preferred here is to decompose three-dimensional advection into three separate one-dimensional flows which act successively upon the evolving tracer distribution. Various names have been applied to this traditional technique: time splitting [*Smolarkiewicz*, 1983], spatial leapfrog [*Russell and Lerner*, 1981], and alternating direction [*Dahlquist and Bjorck*, 1974]. This technique has been applied successfully to two-dimensional transport with second-order moments, as discussed in section 5, and to atmospheric three-dimensional transport with first-order moments [*Russell and Lerner*, 1981]. Potentially, there is a great advantage in the method of alternating directions: concurrent or parallel processors may calculate advection in one-dimension independently (that is, simultaneously) for each set of grid values in the remaining dimensions.

4. One-Dimensional Example With Flux Limitation

Consider the following example of advection of a two-dimensional distribution $f(x, y)$ by the second-order moments method. Let two adjacent boxes, A and B, have equal volumes with unit dimensions ($X = Y = 1$). The tracer mixing ratio is zero everywhere in B,

$$f^B(x, y) = 0 \tag{23}$$

but has a mean value of 100 in A, with a linear slope in the y direction such that

$$f^A(x, y) = 200y \qquad 0 \le y \le 1 \tag{24}$$

Suppose that fluid flow is in the positive x direction, and adopt a time step such that 25% of box A is transported into B. This process is illustrated schematically in one-dimension by Figure 2. The rigorous solution for the second-order moments of the new box B′ is given by the following steps.

Step 1

Define moments of original boxes A and B,

$$\begin{aligned} S_0(\mathrm{A}) &= 100 & S_0(\mathrm{B}) &= 0 \\ S_x(\mathrm{A}) &= 0 & S_x(\mathrm{B}) &= 0 \end{aligned}$$

$$S_{xx}(\mathrm{A}) = 0 \qquad S_{xx}(\mathrm{B}) = 0$$
$$S_{y}(\mathrm{A}) = 100 \qquad S_{y}(\mathrm{B}) = 0$$
$$S_{yy}(\mathrm{A}) = 0 \qquad S_{yy}(\mathrm{B}) = 0$$
$$S_{xy}(\mathrm{A}) = 0 \qquad S_{xy}(\mathrm{B}) = 0$$

Step 2

Calculate moments for appropriate subboxes by (19) and (20),

$$\alpha^{R}(\mathrm{A}) = 0.25 \qquad \alpha^{L}(\mathrm{B}) = 0.75$$
$$S_0{}^{R}(\mathrm{A}) = 25 \qquad S_0{}^{L}(\mathrm{B}) = 0$$
$$S_x{}^{R}(\mathrm{A}) = 0 \qquad S_x{}^{L}(\mathrm{B}) = 0$$
$$S_{xx}{}^{R}(\mathrm{A}) = 0 \qquad S_{xx}{}^{L}(\mathrm{B}) = 0$$
$$S_y{}^{R}(\mathrm{A}) = 25 \qquad \cdots$$
$$S_{yy}{}^{R}(\mathrm{A}) = 0$$
$$S_{xy}{}^{R}(\mathrm{A}) = 0$$

Step 3

Designate components of new grid box B′,

$$S_0{}^{L}(\mathrm{B}') = S_0{}^{R}(\mathrm{A}) \qquad S_0{}^{R}(\mathrm{B}') = S_0{}^{L}(\mathrm{B})$$
$$S_x{}^{L}(\mathrm{B}') = S_x{}^{R}(\mathrm{A}) \qquad S_x{}^{R}(\mathrm{B}') = S_x{}^{L}(\mathrm{B})$$
$$\cdots \qquad \cdots$$

Step 4

Combine subboxes into grid box B′ from (21), $\alpha = \alpha^{R} = 0.75$,

$$S_0(\mathrm{B}') = 25$$
$$S_x(\mathrm{B}') = -56.25$$
$$S_{xx}(\mathrm{B}') = +46.875$$
$$S_y(\mathrm{B}') = 25$$
$$S_{yy}(\mathrm{B}') = 0$$
$$S_{xy}(\mathrm{B}') = -56.25$$

The resulting distribution of tracer is now given by

$$f^{B'}(x, y) = 128.125 - 393.75x + 281.25x^2 + 25(2y - 1) - 56.25(2x - 1)(2y - 1) \qquad (25)$$

Note that advection generates slopes and a cross term S_{xy}, where, originally, there were none. The advective calculation for box B is now complete, unless the velocity field has a y component. In this case, the advection of moments is repeated for an equivalent time step in the y direction.

A desired property of advective methods is often that tracer mixing ratios remain positive even in the vicinity of large discontinuities in tracer abundance. The distribution derived above (25) is negative in some of the permitted domain ($0 \le x \le 1$, $0 \le y \le 1$). Such negative tracer values are clearly an artifact of high-order numerical schemes occurring in the vicinity of large gradients. Many applications of tracer transport, such as photochemical models, cannot accept negative concentrations. It is very difficult to guarantee positive definite values for $f(x, y)$ over the entire domain, so I will address the simpler problem of maintaining a positive average of the tracer distribution in one-dimension,

$$\bar{f}(x) = \int_0^Y \int_0^Z f(x, y, z)\, dy\, dz$$
$$= [(S_0 - S_x + S_{xx}) + (2S_x - 6S_{xx})(x/X) + (6S_{xx})(x/X)^2]/X \qquad (26)$$

where the arbitrary scaling $Y = Z = 1$ has been imposed. The resulting $\bar{f}(x)$ from (25) is illustrated in Figure 2*c* and has a minimum value of $\bar{f}(0.7) = -9.6875$.

In order to maintain positive tracer concentrations, limits are placed on the high-order moments in terms of the total amount of tracer (zeroth moment). This approach leads to some internal diffusion but is not so far reaching as the algorithms used in other schemes to fill in negative tracer amounts from adjacent boxes [*Mahlman and Moxim*, 1978]. The limit procedure is outlined below in greater detail and for this case yields the new moments

$$S_0' = S_0 = 25$$
$$S_x' = -37.5 \qquad (27)$$
$$S_{xx}' = +37.5$$

with a distribution

$$\bar{f}(x) = 100 - 300x + 225x^2 \qquad (28)$$

as shown in Figure 2*d*. The new minimum mixing ratio is now $\bar{f}(2/3) = 0$.

It is difficult to devise a simple algorithm which would guarantee $f(x, y, z) \ge 0$ over the entire volume. Instead, let us require only that the mean tracer distribution along any axis remain positive and that the cross terms by themselves do not produce negative concentrations. Consequently, only positive quantities of tracer are advected. The objective is to place limits on S_x and S_{xx} in order to force $\bar{f}(x)$, as defined in (26), to be positive over the interval $0 \le x \le 1$.

Consider first the case where $S_{xx} < 0$, such that the distribution is convex. The minimum of $\bar{f}(x)$ will occur at either $x = 0$ or $x = 1$:

$$\min f(x) = S_0 - |S_x| - |S_{xx}| \qquad (29)$$

The simplest approach would be to limit the first-order moment to $|S_x| \le S_0$ and to increase the second-order moment so that

$$0 \ge S_{xx} \ge |S_x| - S_0 \qquad (30)$$

The second and more complex case arises for $S_{xx} > 0$, where the distribution is concave. It may be shown that the minimum in $f(x)$ occurs at

$$\min f(x_m) = S_0 - (S_x{}^2 + 3S_{xx}{}^2)/(6S_{xx}) \qquad (31)$$

for

$$x_m = 0.5 - S_x/(6S_{xx}) \qquad (32)$$

If

$$|S_x| > 3S_{xx} > 0 \qquad (33)$$

then the minimum occurs outside the interval, and only the boundaries must be tested. There is some difference here from the first case above in that the second-order moment may offset the first-order moment at the boundary. The algorithm thus places less stringent restrictions on the slope,

$$|S_x| \le 1.5S_0 \qquad (34)$$

```
      SUBROUTINE ADVECT_X(LIMIT)
C        Second-Order Moments Advection of tracer in X-direction
C-----------------------------------------------------------------------
C      The 3-D grid has dimensions  (NX,NY,NZ) with corresponding
C      velocity field (U,V,W).  Parallel subroutines calculate
C      advection in the Y- and Z-directions.
C      The moments [Si] are as defined in the text, SM refers to
C      the total mass in each grid box.
C      The moments [Fi] are similarly defined and used as temporary
C      storage for portions of the grid boxes in transit.
C-----------------------------------------------------------------------
      REAL S0,SX,SXX,SY,SYY,SZ,SZZ,SXY,SXZ,SYZ,SM
      REAL F0,FX,FXX,FY,FYY,FZ,FZZ,FXY,FXZ,FYZ,FM
      REAL U,V,W,DELTAT
      REAL SLPMAX,S1MAX,S1NEW,S2NEW,ALF,ALFQ,ALF1,ALF1Q,TEMPTM
      INTEGER I,J,L,IP1,NX,NY,NZ
      LOGICAL LIMIT
C-----------------------------------------------------------------------
      DIMENSION F0(NX),FX(NX),FY(NX),FZ(NX),FXX(NX),FYY(NX),
     1          FZZ(NX),FXY(NX),FXZ(NX),FYZ(NX),FM(NX)
      COMMON/MOMENTS/ S0(NX,NY,NZ),SX(NX,NY,NZ),SY(NX,NY,NZ),
     1    SZ(NX,NY,NZ),SXX(NX,NY,NZ),SYY(NX,NY,NZ),SZZ(NX,NY,NZ),
     2    SXY(NX,NY,NZ),SYZ(NX,NY,NZ),SXZ(NX,NY,NZ),SM(NX,NY,NZ)
      COMMON/WINDS/ U(NX,NY,NZ),V(NX,NY,NZ),W(NX,NY,NZ),DELTAT
C-----------------------------------------------------------------------
C      Assume periodic boundaries:  (NX,J,L) --> (1,J,L)
C      Mass flux (kg/sec):  U(I,J,L) from  (I,J,L) to (I+1,J,L)
C      Time step:  DELTAT
C-----------------------------------------------------------------------
      DO 50 L=1,NZ
      DO 40 J=1,NY
      IF(.NOT.LIMIT) GOTO 12
C-----------------------------------------------------------------------
C      If flux-limiting transport is to be applied, place limits on
C       appropriate moments before transport.
      DO 10 I=1,NX
      SLPMAX = 0.0
      IF(S0(I,J,L).GT.0.0) SLPMAX = S0(I,J,L)
      S1MAX = 1.5*SLPMAX
      S1NEW = AMIN1( +S1MAX, AMAX1(-S1MAX,SX(I,J,L)) )
      S2NEW = AMIN1( (SLPMAX+SLPMAX-0.3334*ABS(S1NEW)),
     2               AMAX1(ABS(S1NEW)-SLPMAX,SXX(I,J,L)) )
      SXY(I,J,L) = AMIN1( +SLPMAX, AMAX1(-SLPMAX,SXY(I,J,L)) )
      SXZ(I,J,L) = AMIN1( +SLPMAX, AMAX1(-SLPMAX,SXZ(I,J,L)) )
      SX(I,J,L) = S1NEW
   10 SXX(I,J,L) = S2NEW
C-----------------------------------------------------------------------
   12 CONTINUE
C      Readjust moments remaining in the box
      SM(IP1,J,L) = SM(IP1,J,L) - FM(I)
      S0(IP1,J,L) = S0(IP1,J,L) - F0(I)
      SX(IP1,J,L)  = ALF1Q*(SX(IP1,J,L) + 3.*ALF*SXX(IP1,J,L))
      SXX(IP1,J,L) = ALF1*ALF1Q*SXX(IP1,J,L)
      SY(IP1,J,L)  = SY(IP1,J,L) - FY(I)
      SYY(IP1,J,L) = SYY(IP1,J,L) - FYY(I)
      SZ(IP1,J,L)  = SZ(IP1,J,L) - FZ(I)
      SZZ(IP1,J,L) = SZZ(IP1,J,L) - FZZ(I)
      SXY(IP1,J,L) = ALF1Q*SXY(IP1,J,L)
      SXZ(IP1,J,L) = ALF1Q*SXZ(IP1,J,L)
      SYZ(IP1,J,L) = SYZ(IP1,J,L) - FYZ(I)
   26 I = IP1
   28 CONTINUE
C-----------------------------------------------------------------------
C      Put the temporary moments (Fi) into appropriate neighboring boxes
      I = NX
      DO 38 IP1=1,NX
      IF(U(I,J,L).LT.0.0)  GOTO 34
C      Flux from (I) TO (I+1)  when U.GT.0
      SM(IP1,J,L) = SM(IP1,J,L) + FM(I)
      ALF = FM(I)/SM(IP1,J,L)
      ALF1 = 1.0 - ALF
      TEMPTM = ALF*S0(IP1,J,L) - ALF1*F0(I)
      S0(IP1,J,L) = S0(IP1,J,L) + F0(I)
      SXX(IP1,J,L) = ALF*ALF*FXX(I) + ALF1*ALF1*SXX(IP1,J,L)
     2       + 5.*(ALF*ALF1*(SX(IP1,J,L)-FX(I)) - (ALF1-ALF)*TEMPTM)
      SX(IP1,J,L) = ALF*FX(I) + ALF1*SX(IP1,J,L) + 3.*TEMPTM
      SXY(IP1,J,L) = ALF*FXY(I) + ALF1*SXY(IP1,J,L) +
     V                    3.*(-ALF1*FY(I) + ALF*SY(IP1,J,L))
      SXZ(IP1,J,L) = ALF*FXZ(I) + ALF1*SXZ(IP1,J,L) +
     W                    3.*(-ALF1*FZ(I) + ALF*SZ(IP1,J,L))
      SY(IP1,J,L) = SY(IP1,J,L) + FY(I)
      SYY(IP1,J,L) = SYY(IP1,J,L) + FYY(I)
      SZ(IP1,J,L) = SZ(IP1,J,L) + FZ(I)
      SZZ(IP1,J,L) = SZZ(IP1,J,L) + FZZ(I)
      SYZ(IP1,J,L) = SYZ(IP1,J,L) + FYZ(I)
      GOTO 36
C      Flux from (I+1) TO (I)  when U.LT.0
   34 SM(I,J,L) = SM(I,J,L) + FM(I)
      ALF = FM(I)/SM(I,J,L)
      ALF1 = 1.0 - ALF
      TEMPTM = -ALF*S0(I,J,L) + ALF1*F0(I)
      S0(I,J,L) = S0(I,J,L) + F0(I)
      SXX(I,J,L) = ALF*ALF*FXX(I) + ALF1*ALF1*SXX(I,J,L)
     2     + 5.*(ALF*ALF1*(-SX(I,J,L)+FX(I)) + (ALF1-ALF)*TEMPTM)
      SX(I,J,L) = ALF*FX(I) + ALF1*SX(I,J,L) + 3.*TEMPTM
      SXY(I,J,L) = ALF*FXY(I) + ALF1*SXY(I,J,L) +
     V                    3.*(ALF1*FY(I) - ALF*SY(I,J,L))
      SXZ(I,J,L) = ALF*FXZ(I) + ALF1*SXZ(I,J,L) +
     W                    3.*(ALF1*FZ(I) - ALF*SZ(I,J,L))
```

```
C-----------------------------------------------------------------------
C      Calculate flux and moments between boxes (I,J,L) <--> (IP1,J,L)
       I = NX
       DO 28 IP1=1,NX
       IF(U(I,J,L).LT.0.0)  GOTO 24
C       Flux from (I) TO (I+1)  when U.GT.0
C       Create temporary moments/masses for partial boxes in transit
       FM(I) = U(I,J,L)*DELTAT
       ALF = FM(I)/SM(I,J,L)
       ALFQ = ALF*ALF
       ALF1 = 1.0 - ALF
       ALF1Q = ALF1*ALF1
       F0(I) = ALF*(S0(I,J,L) + ALF1*(SX(I,J,L) + (ALF1-ALF)*SXX(I,J,L)))
       FX(I) = ALFQ*(SX(I,J,L) + 3.*ALF1*SXX(I,J,L))
       FXX(I) = ALF*ALFQ*SXX(I,J,L)
       FY(I) = ALF*(SY(I,J,L) + ALF1*SXY(I,J,L))
       FZ(I) = ALF*(SZ(I,J,L) + ALF1*SXZ(I,J,L))
       FXY(I) = ALFQ*SXY(I,J,L)
       FXZ(I) = ALFQ*SXZ(I,J,L)
       FYY(I) = ALF*SYY(I,J,L)
       FZZ(I) = ALF*SZZ(I,J,L)
       FYZ(I) = ALF*SYZ(I,J,L)
C       Readjust moments remaining in the box
       SM(I,J,L) = SM(I,J,L) - FM(I)
       S0(I,J,L) = S0(I,J,L) - F0(I)
       SX(I,J,L)  = ALF1Q*(SX(I,J,L) - 3.*ALF*SXX(I,J,L))
       SXX(I,J,L) = ALF1*ALF1Q*SXX(I,J,L)
       SY(I,J,L)  = SY(I,J,L) - FY(I)
       SYY(I,J,L) = SYY(I,J,L) - FYY(I)
       SZ(I,J,L)  = SZ(I,J,L) - FZ(I)
       SZZ(I,J,L) = SZZ(I,J,L) - FZZ(I)
       SXY(I,J,L) = ALF1Q*SXY(I,J,L)
       SXZ(I,J,L) = ALF1Q*SXZ(I,J,L)
       SYZ(I,J,L) = SYZ(I,J,L) - FYZ(I)
       GOTO 26
C       Flux from (I+1) TO (I)  when U.LT.0
C            (i.e., take left side of box IP1)
   24 FM(I) = -U(I,J,L)*DELTAT
       ALF = FM(I)/SM(IP1,J,L)
       ALFQ = ALF*ALF
       ALF1 = 1.0 - ALF
       ALF1Q = ALF1*ALF1
       F0(I)=ALF*(S0(IP1,J,L)-ALF1*(SX(IP1,J,L)-(ALF1-ALF)*SXX(IP1,J,L)))
       FX(I) = ALFQ*(SX(IP1,J,L) - 3.*ALF1*SXX(IP1,J,L))
       FXX(I) = ALF*ALFQ*SXX(IP1,J,L)
       FY(I) = ALF*(SY(IP1,J,L) - ALF1*SXY(IP1,J,L))
       FZ(I) = ALF*(SZ(IP1,J,L) - ALF1*SXZ(IP1,J,L))
       FXY(I) = ALFQ*SXY(IP1,J,L)
       FXZ(I) = ALFQ*SXZ(IP1,J,L)
       FYY(I) = ALF*SYY(IP1,J,L)
       FZZ(I) = ALF*SZZ(IP1,J,L)
       FYZ(I) = ALF*SYZ(IP1,J,L)
       SY(I,J,L) = SY(I,J,L) + FY(I)
       SYY(I,J,L) = SYY(I,J,L) + FYY(I)
       SZ(I,J,L) = SZ(I,J,L) + FZ(I)
       SZZ(I,J,L) = SZZ(I,J,L) + FZZ(I)
       SYZ(I,J,L) = SYZ(I,J,L) + FYZ(I)
   36 I = IP1
   38 CONTINUE
C-----------------------------------------------------------------------
   40 CONTINUE
   50 CONTINUE
      RETURN
      END
```

Fig. 1. FORTRAN subroutine which performs the advection of tracer in the x-direction conserving second-order moments.

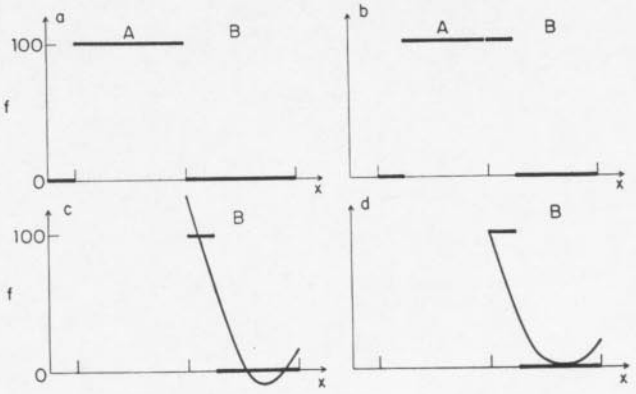

Fig. 2. The mixing ratio of tracer f in one spatial dimension x is shown (a) before and (b) after an advective time step which transports 25% of the contents of boxes A and B in the positive x-direction. The smooth polynomial distribution of the tracer, which corresponds to the moments of the two discontinuous subintervals in B is shown (c) before and (d) after limits are placed to ensure positive tracer concentrations.

and uses the second-order moment to fill in negative values,

$$S_{xx} \geq |S_x| - S_0 \tag{35}$$

The other branch of the second case occurs when the second-order moment dominates the slope,

$$3S_{xx} \geq |S_x| > 0 \tag{36}$$

and a minimum occurs within the interval. If the limit (34) is first placed on S_x, it can be shown that $\bar{f}(x) \geq 0$ if

$$S_{xx} \leq S_{xx}{}^{\max} = S_0 + [S_0{}^2 - S_x{}^2/3]^{1/2} \tag{37}$$

It may be undesirable to calculate a square root at each advective time step, and a simpler but more restrictive formula may be used.

$$S_{xx} \leq 2S_0 - |S_x|/3 < S_{xx}{}^{\max} \tag{38}$$

These limit cases, along with the restriction on cross terms, may be combined into a few tests,

$$\begin{aligned} S_0 &\geq 0 \\ S_x' &= \min\,[+1.5S_0,\ \max\,(-1.5S_0,\ S_x)] \\ S_{xx}' &= \min\,[2S_0 - |S_x'|/3,\ \max\,(|S_x'| - S_0,\ S_{xx})] \\ S_{xy}' &= \min\,[+S_0,\ \max\,(-S_0,\ S_{xy})] \end{aligned} \tag{39}$$

where the primed quantities have been corrected. While these manipulations may seem arbitrary, they are applied only in the most severe cases, as given in the example. Generally, the tracer distribution will evolve to a state where the limits imposed in (39) should not affect the moments. The second-order moments method may be applied without these limits if negative tracer concentrations can be accommodated.

5. Accuracy, Stability, and Resolution

The accuracy and stability of the second-order moments method may be derived analytically for the case of uniform, one-dimensional transport over an equally spaced grid. Let the tracer distribution be decomposed into Fourier components and examine the advective transport of one such wave,

$$f(x) = e^{ikx} \tag{40}$$

For the grid box $0 \leq x \leq X$, the moments may be calculated from (11)

$$\begin{aligned} S_0 &= X(e^{ikX} - 1)/(ikX) \\ S_x &= 6X[(e^{ikX} + 1)/2 - (e^{ikX} - 1)/(ikX)]/(ikX) \\ S_{xx} &= 5X\{(e^{ikX} - 1)[1 + 12/(ikX)^2] - 6(e^{ikX} + 1)/(ikX)\}/(ikX) \end{aligned} \tag{41}$$

The moments for the previous grid box ($-X \leq x \leq 0$) can be calculated by multiplying the respective moments in (41) above by the phase shift factor e^{-ikX}. Now consider a uniform velocity c and time step t with $\alpha = ct/X$ as before. The true values after one time step are

$$S_j{}^{\text{true}}(t) = e^{-ikX\alpha} S_j(0) \qquad j = 0,\ x,\ xx \tag{42}$$

whereas the calculated moments $S_j{}^{\text{calc}}(t)$ can be shown to have the following errors:

$$\begin{aligned} S_0{}^{\text{calc}}(t) &= S_0{}^{\text{true}}(t) + X(ikX)^4(\alpha - 6\alpha^2 + 10\alpha^3 - 5\alpha^4)/120 \\ &\quad + X(ikX)^5(\alpha - 10\alpha^2 + 30\alpha^3 - 35\alpha^4 + 14\alpha^5)/1680 + \text{order}[(ikX)^6] \end{aligned} \tag{43a}$$

$$\begin{aligned} S_x{}^{\text{calc}}(t) &= S_x{}^{\text{true}}(t) + X(ikX)^3(\alpha - 6\alpha^2 + 10\alpha^3 - 5\alpha^4)/20 \\ &\quad + X(ikX)^4(\alpha - 3\alpha^2 + 2\alpha^3)/280 + \text{order}[(ikX)^5] \end{aligned} \tag{43b}$$

$$\begin{aligned} S_{xx}{}^{\text{calc}}(t) &= S_{xx}{}^{\text{true}}(t) + X(ikX)^3(\alpha^2 - 4\alpha^3 + 5\alpha^4 - 2\alpha^5)/4 \\ &\quad + X(ikX)^4(7\alpha - 39\alpha^2 + 64\alpha^3 - 32\alpha^4)/168 + \text{order}[(ikX)^5] \end{aligned} \tag{43c}$$

Note that the errors disappear for $\alpha = 0$ or $\alpha = 1$, as expected for upstream methods. The complex ratio

$$S_j{}^{\text{calc}}(t)/S_j(0) = Ae^{iB} \tag{44}$$

gives a measure of both the amplification factor A and the computed phase speed of the wave ($c_{\text{phase}} = -B/kt$). Table 1 shows the amplification factors and relative phase speeds (c_{phase}/c) for the allowed domain: $0 < \alpha < 1$, $0 < kX \leq \pi$. For S_0 the method is absolutely stable ($A \leq 1$) only for a restricted range of α

$$0.2764 < \alpha < 0.7236 \tag{45}$$

However, it is only marginally unstable over the rest of the domain, with a worst case instance of $A = 1.03$ for $\alpha = 0.85$ and $kX = \pi$. In those cases where S_0 is stable, the higher-order moments S_x and S_{xx} are marginally unstable, and vice versa. Phase errors are extremely small, with the exception of a combination of small α and values of kX near π (that is, Nyquist frequency).

An important measure of any advective scheme is the effective resolution of the method: how many grid points are needed to resolve a structure? One test is the advection of a step function:

$$f(x, y, z) = 1 \qquad x < x_0 \qquad y < y_0 \qquad z < z_0 \tag{46}$$

elsewhere,

$$f(x, y, z) = 0$$

Examples of one-, two-, and three-dimensional uniform flows are presented in Figure 3 for the second-order moments method and its lower-order forms, the slopes method [*Russell and Lerner*, 1981], and plain upstream advection. The discontinuous function (46) rapidly changes into a shape which the algorithm can accurately describe and transport across the grid. Subsequently, this quasi-static shape continues to evolve

TABLE 1. Amplification Factors and Relative Phase Speeds From the Second-Order Moments Method

	kX/π				
ct/X	0.05	0.25	0.50	0.75	1.00
			Amplification, S_0		
0.10	1.000	1.000	1.002	1.011	1.028
0.30	1.000	1.000	0.999	0.996	0.983
0.50	1.000	1.000	0.996	0.980	0.920
0.70	1.000	1.000	0.999	0.996	0.983
0.90	1.000	1.000	1.002	1.011	1.028
1.00	1.000	1.000	1.000	1.000	1.000
			Relative Phase, S_0		
0.10	1.000	1.001	1.010	1.051	1.179
0.30	1.000	1.000	1.000	1.001	1.001
0.50	1.000	1.000	1.000	1.000	1.000
0.70	1.000	1.000	1.000	1.000	0.999
0.90	1.000	1.000	0.999	0.994	0.980
1.00	1.000	1.000	1.000	1.000	1.000
			Amplification, S_x		
0.10	1.000	0.997	0.988	0.975	0.962
0.30	1.000	1.001	1.002	1.002	0.997
0.50	1.000	1.004	1.016	1.040	1.080
0.70	1.000	1.001	1.002	1.002	0.997
0.90	1.000	0.997	0.988	0.975	0.962
1.00	1.000	1.000	1.000	1.000	1.000
			Relative Phase, S_x		
0.10	1.000	0.991	0.962	0.908	0.822
0.30	1.000	1.002	1.007	1.016	1.029
0.50	1.000	1.000	1.000	1.000	1.000
0.70	1.000	0.999	0.997	0.993	0.988
0.90	1.000	1.001	1.004	1.010	1.020
1.00	1.000	1.000	1.000	1.000	1.000
			Amplification, S_{xx}		
0.10	1.000	0.989	0.966	0.959	1.024
0.30	1.000	1.005	1.020	1.048	1.093
0.50	1.000	1.011	1.046	1.110	1.211
0.70	1.000	1.005	1.020	1.048	1.093
0.90	1.000	0.989	0.966	0.959	1.024
1.00	1.000	1.000	1.000	1.000	1.000
			Relative Phase, S_{xx}		
0.10	0.807	0.745	0.565	0.283	−0.012
0.30	0.827	0.823	0.821	0.818	0.815
0.50	1.000	1.000	1.000	1.000	1.000
0.70	1.074	1.076	1.077	1.078	1.079
0.90	1.021	1.028	1.048	1.080	1.110
1.00	1.000	1.000	1.000	1.000	1.000

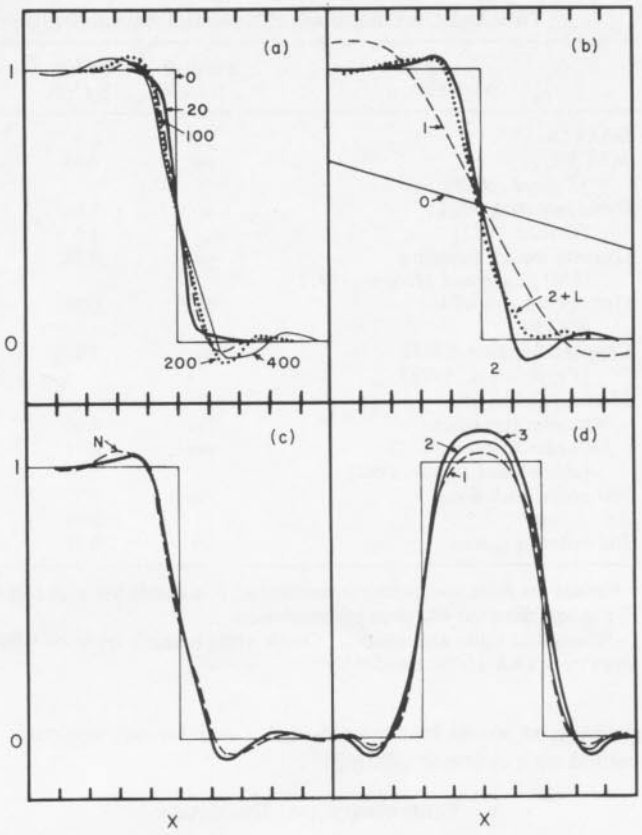

Fig. 3. Tracer mixing ratios f are shown for numerical advection of a step function (see text). (*a*) The evolution of the initial step function at time zero (labeled 0) following one-dimensional advection by the second-order moments (SOM) method through 20, 100, 200, and 400 grid intervals with a Courant step size of $ct/X = 0.20$. (*b*) The basic upstream advective scheme (0), the slopes or first-order moments method (1), the SOM method with limits (2 + L) and without limits (2) are compared. The step function has been advected in one dimension across 200 grid boxes with a Courant step of 0.20. (*c*) The effect of "checkerboard" noise N on SOM for the same case as Figure 3*b* above. (*d*) Results from the one-dimensional (1), two-dimensional (2), and three-dimensional (3) advection of a $4 \times 4 \times 4$ cube of tracer. The Courant step sizes were 1/2, 1/3, 1/6 for the (x, y, z) directions, and the advection was followed for 96 steps. The mixing ratio shown in Figure 3*d* is along an axis through the center of the cube.

slowly and stably. The slopes scheme is capable of resolving a step function with four to five grid points in one-dimension; whereas the second-order moments method can maintain a step function with only two grid points. As can be seen in Figure 3, the imposition of limits (39) adds only minor numerical diffusion.

Upstream methods have already been noted to do extremely well under conditions of noisy flow [*Russell and Lerner*, 1981]. As an additional test which includes divergent flows, the two-dimensional (i, j)-grid is considered as a checkerboard in which the "black" squares ($i + j$ odd) collect mass from all neighboring "red" squares ($i + j$ even) for several time steps, following which the process reverses. This oscillating two-point grid noise is imposed on top of the uniform flow used above and has an amplitude (50%) such that the density of each grid box varies by a factor of 2 over the cycle. As shown in Figure 2, such noisy flows do not significantly affect the one-dimensional advection of the step function. The accuracy of two-dimensional flows is reduced (errors of order 25%) when the noise level exceeds 50%, but it is not noticeably affected (errors less than 2%) when the noise in the mean flow is 10% of the grid box mass.

There are questions of stability in such a complex scheme when operator splitting is used to calculate multidimensional advection. A test proposed by one of the reviewers includes convergent/divergent flow in the x direction, which is balanced by flow in the y direction:

$$u(x, y) = a(2\pi/Y) \sin(2\pi x/X) \cos(2\pi y/Y)$$
$$v(x, y) = -a(2\pi/X) \cos(2\pi x/X) \sin(2\pi y/Y) \tag{47}$$

In this case the entire domain is limited by $0 < x < X$ and $0 < y < Y$, and the amplitude a must be small enough so that no grid box acquires a negative density during the advective time step assigned to each dimension. Beginning with a uniform grid of total mass and tracer mixing ratio, advection according to (47) by the second-order moments method with operator splitting preserves the tracer uniformity to machine

TABLE 2. A Comparison of Numerical Advection Algorithms: The "Clock" Experiment From *Chock and Dunker* [1983]

Method	Positive Tracer	$\Sigma f^2(t)/\Sigma f^2(0)$	Average |Error|	Maximum |Error|	Time Step, π	CPU,* s	Two-dimensional Arrays
SHASTA	yes	0.3	1.4	75	15	44	4
MFCT/LT	yes	0.55	0.7	47	15	140	8
[*Zalesak*, 1979]							
Pseudospectral (PS/L)	no	1.0	0.3	8	15	190	6
[*Orszag*, 1972]		1.0	0.10	2	5	570	6
Discrete second moments	yes	0.78	0.6	38	15	190	12
(SM) [*Egan and Mahoney*, 1972]							
Orthogonal collocation	no	0.96	3.2	58	15	63	7
(OC/PC)							
Chapeau function (CF/I)	no	1.0	0.9	22	15	51	3
[*Pepper et al.*, 1979]							
Moments Methods							
0th order (upstream)	yes	0.04	2.4	95	15	19	1
1st order with limits	yes	0.71	0.40	24	15	67	3
[*Russell and Lerner*, 1981]		0.80	0.26	14	60	17	3
2nd order, with limits	yes	0.97	0.06	2	15	102	6
		0.96	0.05	2	60	26	6
2nd order, no limits	no	0.98	0.07	2	60	24	6

Results are from two complete revolutions of a cosine hill with half-height radius of 2 grid boxes and an original height of 100. A time step of 15 π is equivalent to 480 steps per revolution.

*Computer times are based on Chock and Dunker's reported CPU seconds for an IBM 3033; timings for the moments methods are CPU times on a VAX 11/780 divided by 7.

accuracy, as would be expected in this case for any upstream method with operator splitting.

6. Comparison and Discussion

The second-order moments method is summarized by (19), (20), and (21), with the optional limit condition (39). The initial distribution of tracer is decomposed into moments S_i over a set of connected grid boxes. Only the mean concentrations (S_0/V) need be specified to start; high-order moments may be zero. A specific time step for each dimension is selected from the globally limiting value of the Courant number. The grid boxes are cleaved (along the remaining dimensions) into appropriate subunits to be transported to and from adjacent boxes. The moments of the tracer distribution are subdivided according to (19)–(20) and then recombined within the appropriate new grid boxes according to (21). If limits are imposed, formulae (39) are invoked prior to decomposition by (19)–(20). This process is repeated for the remaining dimensions to complete the advective time step.

The second-order moments method may be compared with several other methods reviewed in the literature. Advection of a parcel of tracer in a rigidly rotating plane would appear to provide a useful cross comparison of methods. *Chock and Dunker* [1983] selected a cosine hill of tracer with a radius of 4 units at a distance of 10 units from the center of a 33 × 33 unit grid. Results from several methods tested by this "clock" experiment are compared in Table 2 with calculations using the upstream moments method. Some criteria for selection of numerical methods are given in Table 2: (1) nonnegative tracer concentrations, (2) low numerical diffusion (Σf^2), (3) low average absolute error, (4) low values for the maximum error at any point, (5) computational time, and (6) storage requirements for two-dimensional arrays.

If we require that tracer concentrations remain nonnegative, then, among those listed by *Chock and Dunker* [1983], only flux-correction methods (SHASTA, MFCT/LT) or the discrete second-moments method [*Egan and Mahoney*, 1972] are acceptable. When compared with these generally more diffusive methods, it may be seen that even the first-order moments method [*Russell and Lerner*, 1981] is superior in terms of accuracy and computational efficiency. The second-order moments method, however, provides an order of magnitude reduction in the diffusion and absolute error, with only small additional costs in programming, computation, and storage. It should be noted that the cross moments (S_{xy}) are essential to the stability of the scheme.

If the major requirement of an advective scheme is absolute accuracy, then pseudospectral methods [*Orszag*, 1972] or the Chapeau function method must be selected from *Chock and Dunker*'s [1983] examples. Compared with this class of algorithms, the second-order moments method may be marginally more dispersive (0.96 versus 1.0), but it is significantly more accurate in terms of average or maximum errors. Application of this method without limits reduces the numerical diffusion but results in negative tracer concentrations.

A further advantage of the second-order moments method is that the time step may be increased by a factor of 4 ($\Delta t = 60\pi$, computer time = 24 s) without degrading accuracy. Indeed, if the same level of accuracy were required from the only other method capable of such skill, the pseudospectral method, then the time step would have to be divided by 3 ($\Delta t = 5\pi$, time = 570 s), and the relative cost in computation would be greater by a factor of about 24.

A revised form of upstream transport with an antidiffusive step has been proposed by *Smolarkiewicz* [1983]. His test case used a cone of radius of 15 units at a distance of 25 units from the center of a 100 × 100 unit grid. After six revolutions, he examines (1) the peak value of the cone and (2) the dispersion error, as shown in Table 3. The second-order moments method is seen to reduce both errors by at least an order of magnitude.

Schneider [1984] has proposed a square root scheme for advection which dramatically improves the accuracy of traditional finite difference methods while maintaining positive tracer concentrations. I repeated his example of the one-dimensional transport of a triangular wedge of height 1.00 resolved by 10 grid points. Schneider's Figure 2*e* shows errors of order ± 0.2 across the wedge; whereas the second-order

TABLE 3. A Comparison of Algorithms From *Smolarkiewicz* [1983]

Method	Peak Value	Dispersion Error
Upstream	0.07	0.95
FCT	0.79	0.29
Modified upstream		
[(19)(20)]	0.60	0.52
$[(13)(14)^3]/TS$	0.84	0.13
Second-order moments	0.99	0.002

The labeling and notation in this table are those of *Smolarkiewicz* [1983]. The FCT method appears to be equivalent to the MFCT method used by *Chock and Dunker* [1983]. Smolarkiewicz's optimal scheme is given by $[(13)(14)^3]/TS$. The original, conelike distribution has a peak value of 1.00 with a radius of 15 grid units and is allowed to revolve 6 times. The dispersion error is the complement of the dispersion defined in Table 2: $1 - \Sigma f^2(t)/\Sigma f^2(0)$.

moments method with limits has errors of -0.05 at the central peak and less than ± 0.02 everywhere else.

These examples are restricted in scope; a more interesting test would examine the dispersion of tracer distribution in a realistic three-dimensional divergent flow. *Russell and Lerner* [1981] have compared the slopes (first-order moments) method with traditional second- and fourth-order differencing methods in several experiments, including a three-dimensional tracer model of the atmosphere. They find that slopes and fourth-order methods are equivalent for uniform grids but that the slopes method is superior for irregular grids (a common property in atmospheric models). As noted in section 5, the second-order moments scheme shares these advantages with the slopes scheme and should provide increased accuracy with significantly lower numerical diffusion (see Tables 2 and 3).

In summary, a new method for advection of trace species is presented and shown to be superior to most available methods in terms of accuracy, numerical diffusion, and computational cost. The method is based on conservation of the second-order moments of the tracer distribution about the center of mass in each grid box. The second-order moments method has, in addition, three characteristics which are useful when applied to atmospheric tracer models: positive tracer concentrations can be maintained, large time steps do not significantly reduce accuracy, and spatial and temporal fluctuations in grid box volumes are readily included.

Acknowledgments. I would like to thank my colleagues, especially C. Spivakovsky, without whose discussions and encouragement this work would not have been written. This research was supported by National Aeronautic and Space Administration grant NAGW-359, National Science Foundation grant ATM-81-17009, and Coordinating Research Council grant CAPA-22-83.

REFERENCES

Chock, D. P., and A. M. Dunker, A comparison of numerical methods for solving the advection equation, *Atmos. Environ.*, *17*, 11–24, 1983.

Dahlquist, G., and A. Bjorck, *Numerical Methods*, Prentice Hall, Englewood Cliffs, N. J., 1974.

Egan, B. A., and J. R. Mahoney, Numerical modelling of advection and diffusion of urban-area source pollutants, *J. Appl. Meteorol.*, *11*, 312–322, 1972.

Eliassen, A., A review of long-range transport modeling, *J. Appl. Meteorol.*, *19*, 231–240, 1980.

Fung, I., K. Prentice, E. Matthews, J. Lerner, and G. Russell, Three-dimensional tracer model study of atmospheric CO_2: Response to seasonal exchanges with the terrestrial biosphere, *J. Geophys. Res.*, *88*, 1379–1400, 1983.

Graedel, T. E., and J. A. Schiavone, 2-D studies of the kinetic photochemistry of the urban troposphere, II, Normal convective conditions, *Atmos. Environ.*, *15*, 353–361, 1981.

Haltiner, G. J., and R. T. Williams, *Numerical Prediction and Dynamic Meteorology*, John Wiley, New York, 1980.

Holton, J. R., An advective model for two-dimensional transport of stratospheric trace species, *J. Geophys. Res.*, *86*, 11,989–11,994, 1981.

Ko, M. K. W., N. D. Sze, M. Livshits, M. B. McElroy, and J. A. Pyle, The seasonal and latitudinal behavior of trace gases and ozone as simulated by a two-dimensional model of the atmosphere, *J. Atmos. Sci.*, *41*, 2381–2408, 1984.

Levy, H., II, J. D. Mahlman, and W. J. Moxim, Tropospheric N_2O variability, *J. Geophys. Res.*, *87*, 3061–3080, 1982.

Mahlman, J. D., and W. J. Moxim, Tracer simulation using a global general circulation model: Results from a mid-latitude instantaneous source experiment, *J. Atmos. Sci.*, *35*, 1340–1374, 1978.

Mahlman, J. D., and R. W. Sinclair, Test of various numerical algorithms applied to a simple trace constituent air transport problem, in *Fate of Pollutants in the Air and Water Environments*, edited by I. H. Suffet, pp. 223–252, John Wiley, New York, 1977.

McRae, G. J., and J. H. Seinfeld, Development of a second-generation mathematical model for urban air pollution, II, Evaluation of model performance, *Atmos. Environ.*, *17*, 501–522, 1983.

McRae, G. J., W. R. Goodin, and J. H. Seinfeld, Development of a second-generation mathematical model for urban air pollution, I, Model formulation, *Atmos. Environ.*, *16*, 679–696, 1982.

Orszag, S. A., Comparison of pseudo-spectral and spectral approximation, *Stud. Appl. Math.*, *51*, 253–259, 1972.

Pepper, D. W., C. D. Kern, and P. E. Long, Modeling the dispersion of atmospheric pollution using cubic splines and chapeau functions, *Atmos. Environ.*, *13*, 223–237, 1979.

Russell, G. L., and J. A. Lerner, A new finite-differencing scheme for the tracer transport equation, *J. Appl. Meteorol.*, *20*, 1483–1498, 1981.

Schere, K. L., An evaluation of several numerical advection schemes, *Atmos. Environ.*, *17*, 1897–1907, 1983.

Schneider, H. R., A numerical transport scheme which avoids negative mixing ratios, *Mon. Weather Rev.*, *112*, 1206–1217, 1984.

Seinfeld, J. H., *Air Pollution: Physical and Chemical Fundamentals*, McGraw-Hill, New York, 1975.

Smolarkiewicz, P. K., A simple positive definite advection scheme with small implicit diffusion, *Mon. Weather Rev.*, *111*, 479–486, 1983.

Smolarkiewicz, P. K., A fully multidimensional positive definite advection algorithm with small implicit diffusion, *J. Comp. Phys.*, *54*, 325–362, 1984.

Steed, J. M., A. J. Owens, C. Miller, D. L. Filkin, and J. P. Jesson, Two-dimensional modelling of potential ozone perturbations by chlorofluorocarbons, *Nature*, *295*, 308–311, 1982.

Tung, K. K., On the two-dimensional transport of stratospheric trace gases in isentropic coordinates, *J. Atmos. Sci.*, *39*, 2330–2355, 1982.

Zalesak, S. T., Fully multidimensional flux-corrected transport algorithms for fluids, *J. Comp. Phys.*, *31*, 335–362, 1979.

M. J. Prather, NASA Goddard Institute for Space Studies, 2880 Broadway, New York, NY 10025.

(Received August 20, 1984;
revised February 11, 1986;
accepted February 12, 1986.)